Particle identification of relativistic heavy ions

Chiara Nociforo

GSI Helmholtzzentrum für Schwerionenforschung
Darmstadt - Germany

IDPASC School – Siena – 2013 Oct 4-6

Contents

- Introduction of in-flight production of rare isotope beams (RIBs)

    production, selection and separation method

    GSI facilties: FRS vs Super-FRS

- Particle identification of relativistic ions

    standard PID detectors

    new requirements & developments

- Unique experiments

Chart of nuclides

About 6000 nuclides are bound, only about half of them have been observed. Most of the unobserved nuclides are neutron-rich.

Experimental progress on nuclear structure relies on available beams of nuclei far from stability.

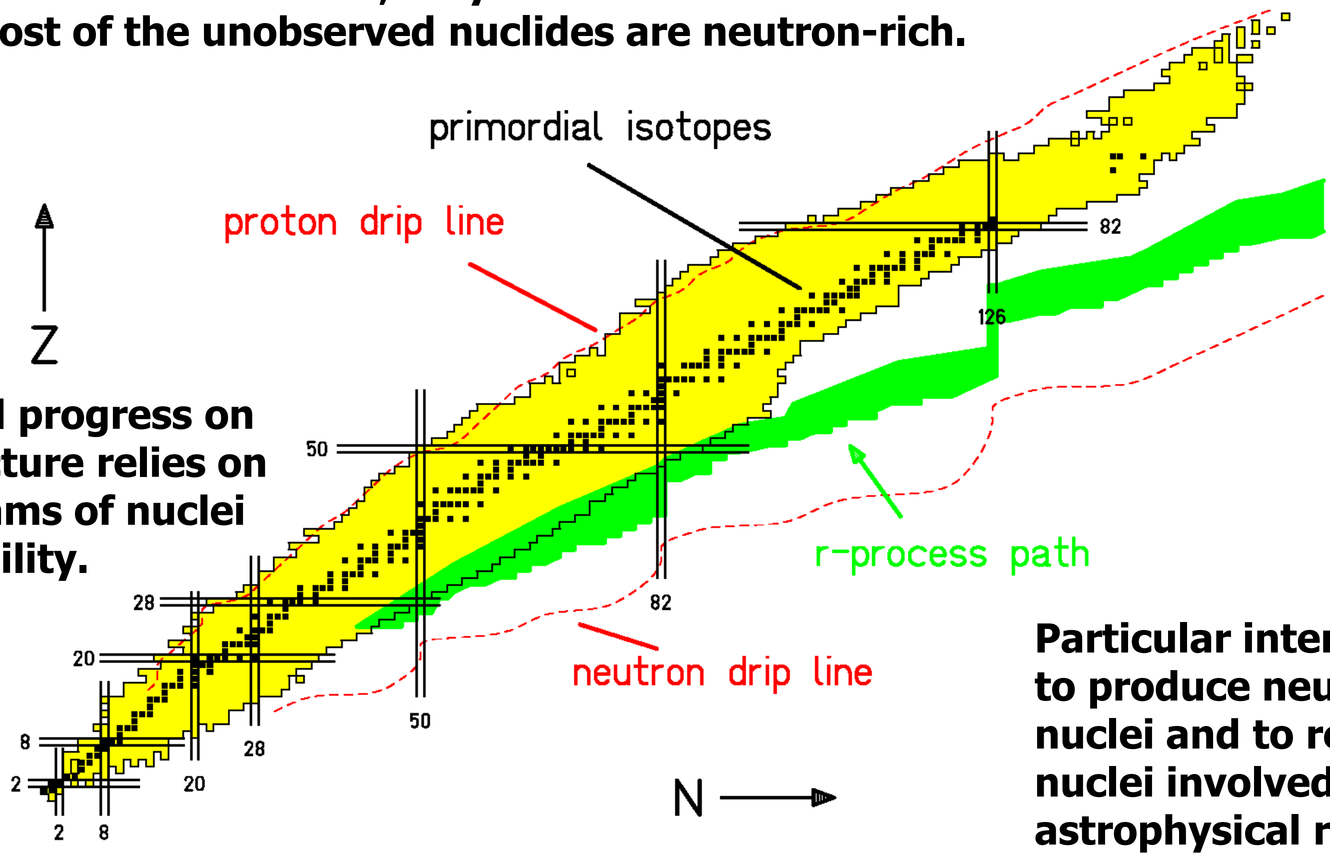

Particular interest to produce neutron-rich nuclei and to reach the nuclei involved in the astrophysical r-process.

http://www-win.gsi.de/charms/euro2000.htm

Basic method: production

1 nuclear physics:

reaction kinematics
production cross sections
nuclear absorption

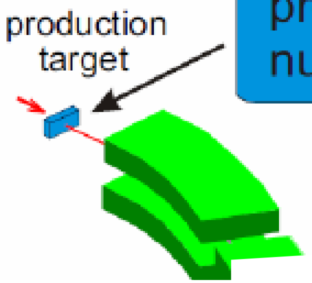

E_{proj} ~ 100-1000 MeV/u , λ ~ 2-0.2 fm

Nucler reactions to produce RIBs

- fragmentation
- spallation
- fission
- fusion
- transfer

High Energy

High and Low Energy

Thick target (few g/cm²) to increase the yields $Y(Z,A) = N_t \, I_{proj} \, \sigma(Z,A) \, \varepsilon$

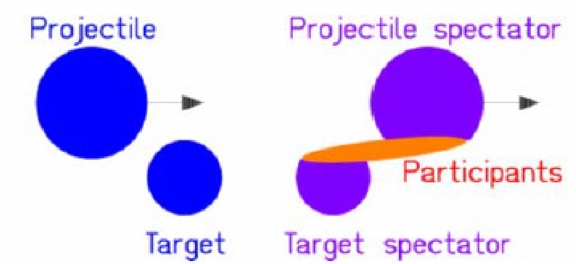

$v_{frag} \sim v_{proj}$

I_{proj} : N_{proj} / s

cross section

transmission, selection and efficency

Basic method: selection

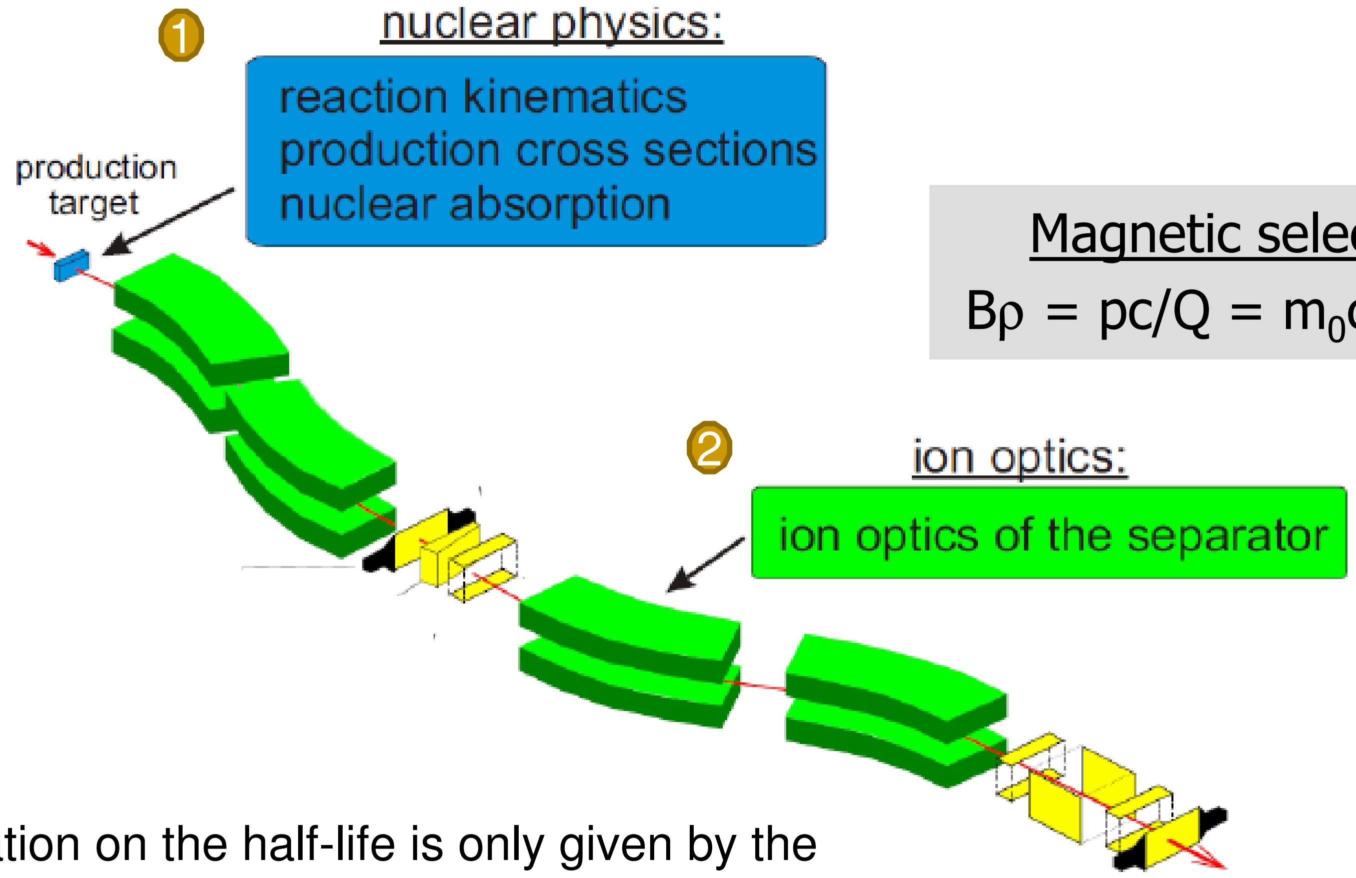

Magnetic selection

$B\rho = pc/Q = m_0c^2\beta\,\gamma/Q$

Limitation on the half-life is only given by the flight time of the ions through the device.

Separation method
momentum-loss-achromat

Because the fragments have approximately the same velocity they will loose different momenta in the degrader depending on their atomic number Z and will exit with different magnetic rigidity.

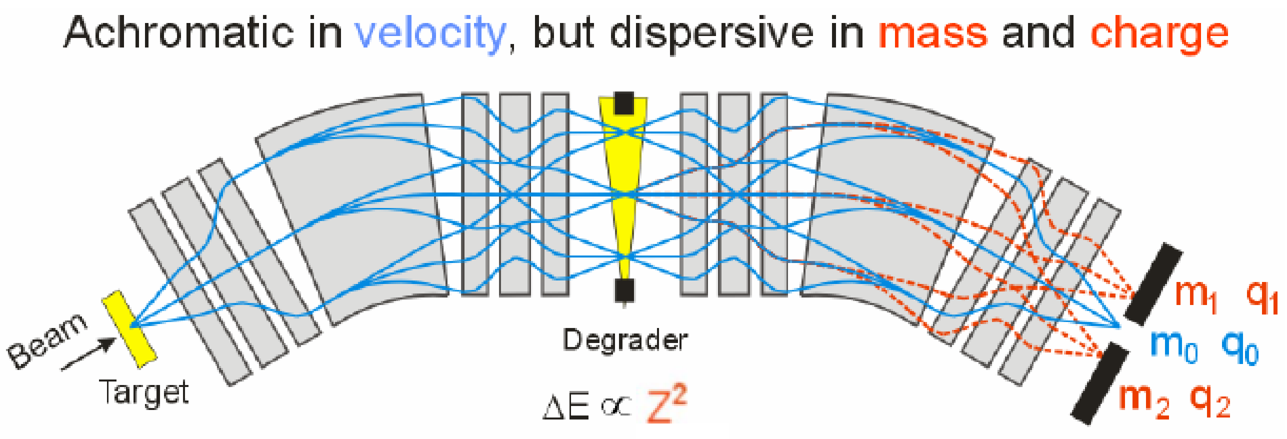

The final position and angle do not depend on momentum.

J.P. Dufour et al. *NIM A* 248 (1986) 267
K.-H. Schmidt et al. *NIM A* 260 (1987) 287

Degraders

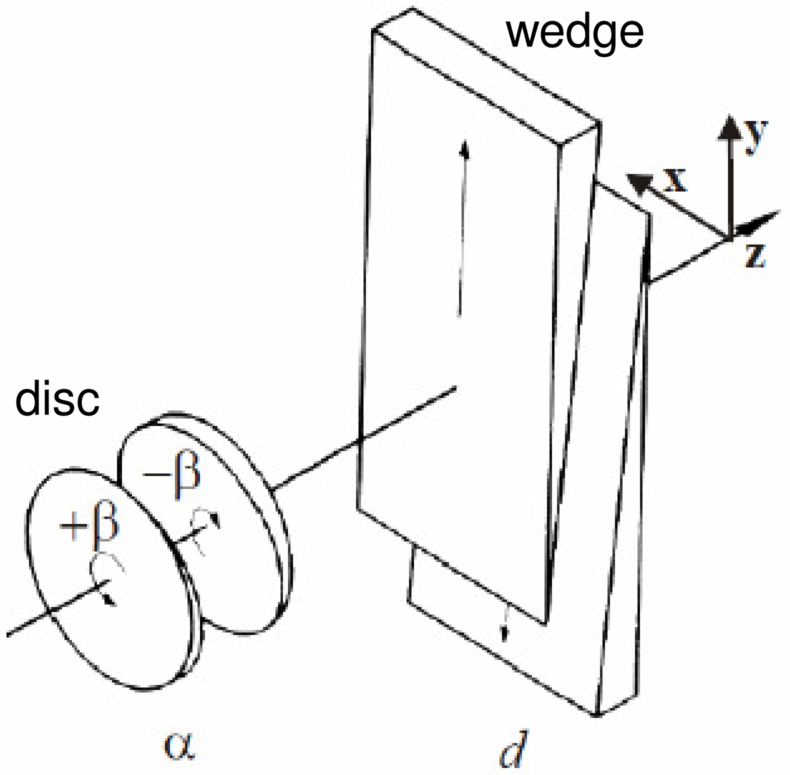

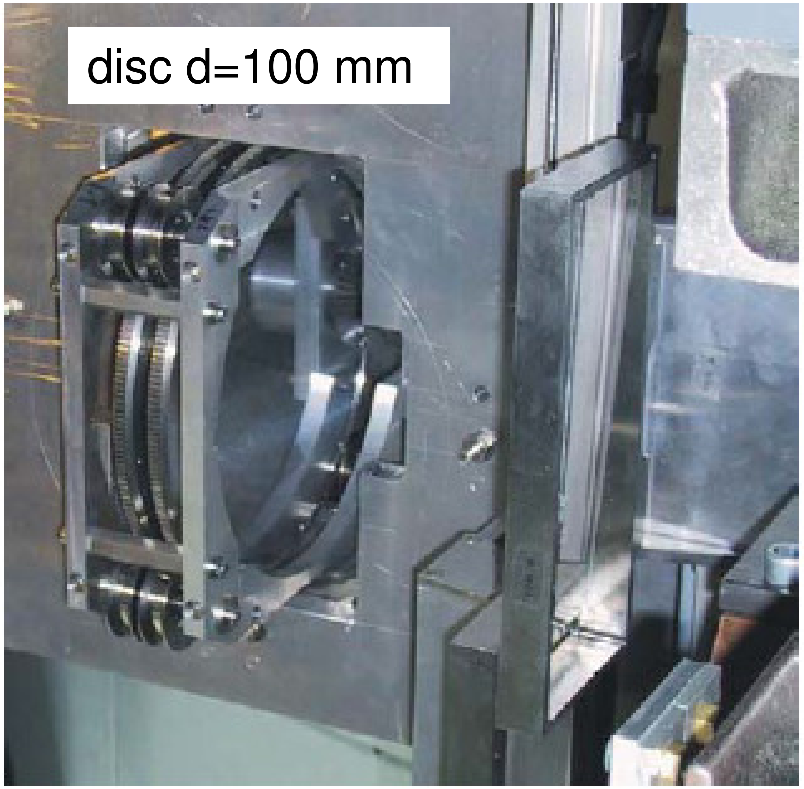

Wedge shaped disc and double-shaped wedge machined with μm precision

Basic method: separation

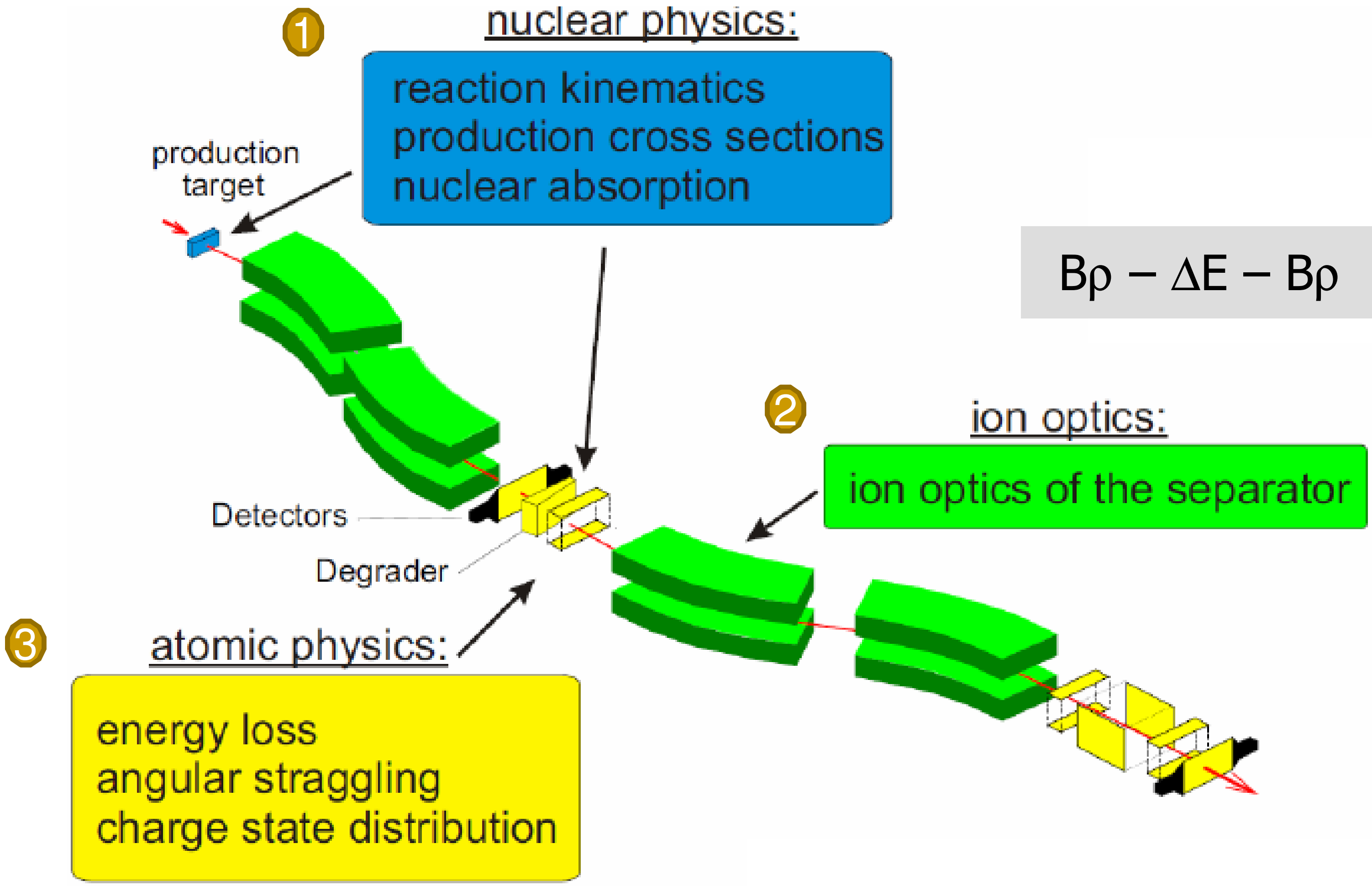

$B\rho - \Delta E - B\rho$ method

GSI Accelerator Facility

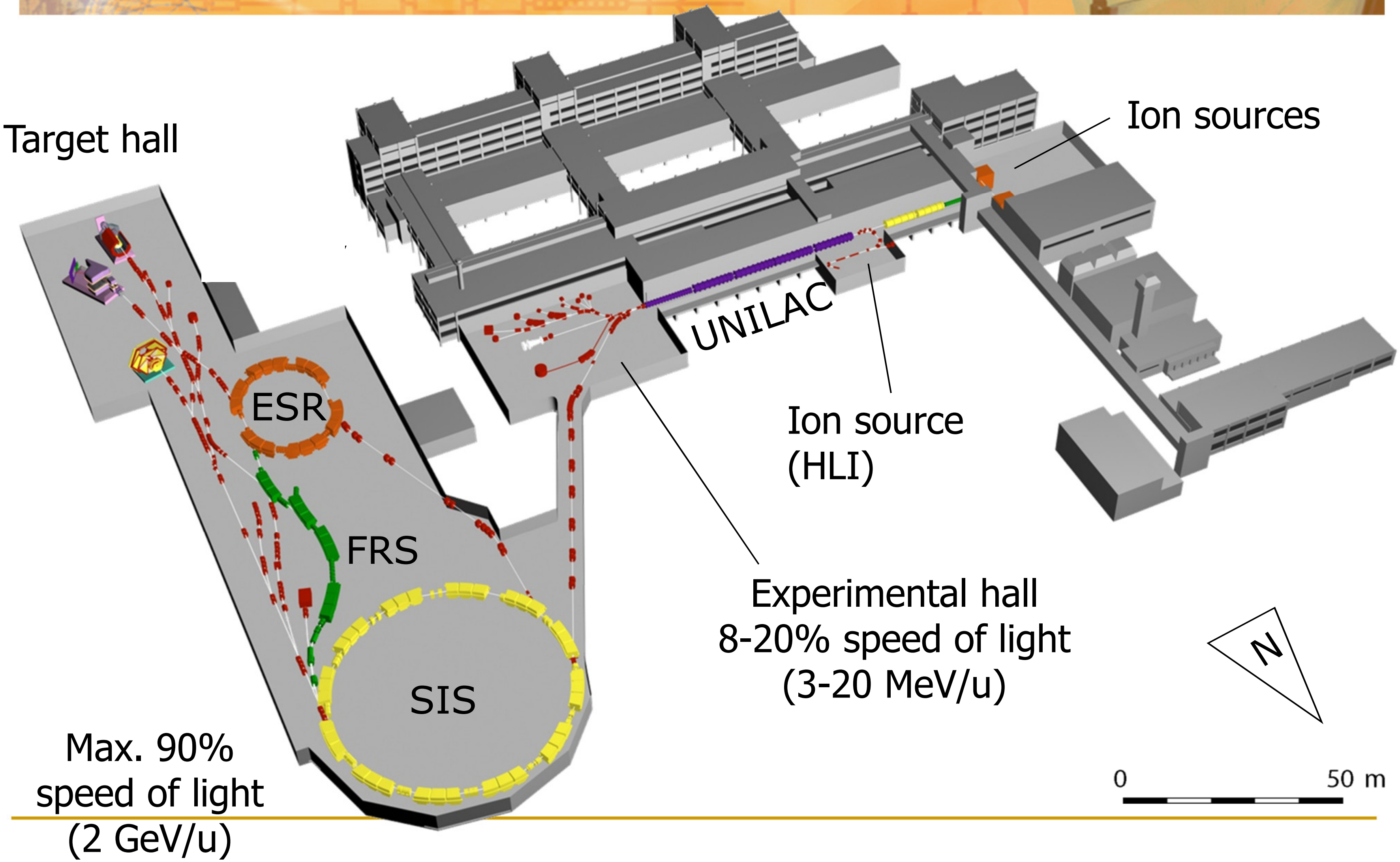

FRagment Separator

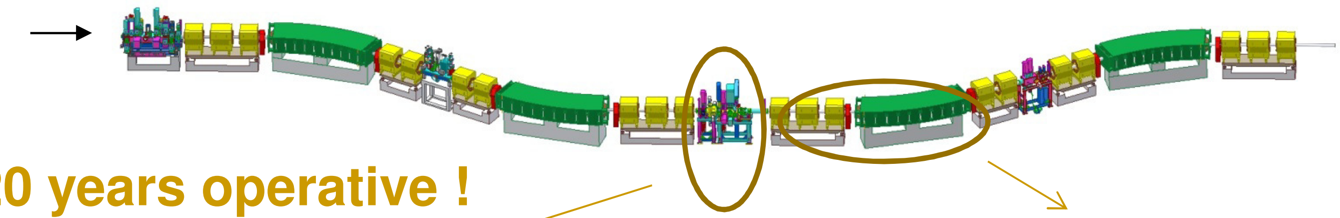

Since 20 years operative !

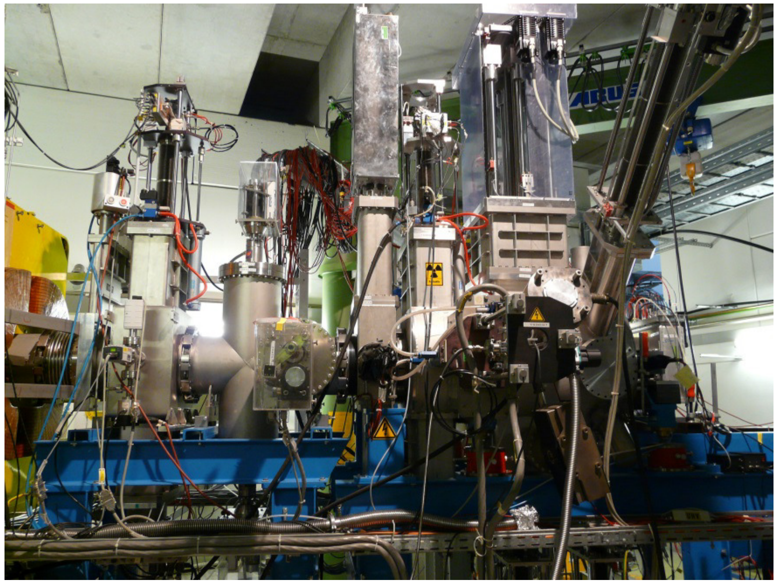

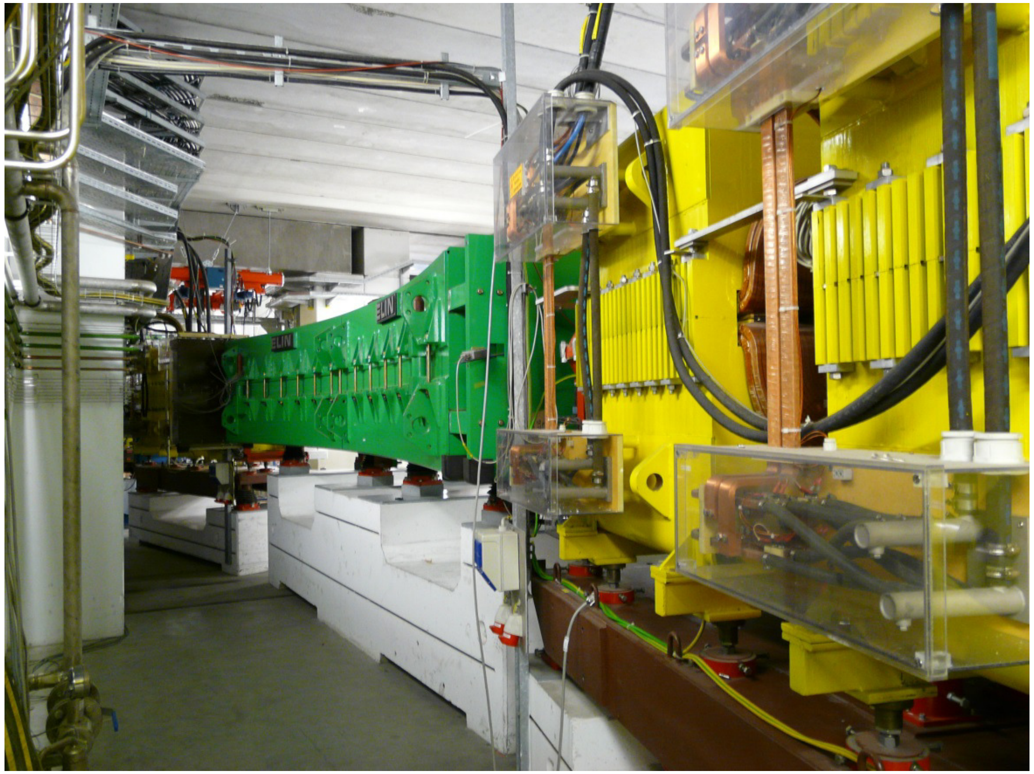

H. Geissel et al. *NIM B* 204 (2003) 71

In-flight PID

$Z \leftarrow \; -dE/dx = \mathrm{f}\,(Z, \beta)$ atomic number

$$A/Q = \frac{B\rho}{\gamma\beta m_u}$$

Z ≠ Q charge state

$$A = \frac{T_{\mathrm{KE}}}{(\gamma - 1)\, m_u}$$

mass number, T_{KE} kinetic energy

$$Q = \frac{A}{A/Q}$$

Bρ – ToF – ΔE method

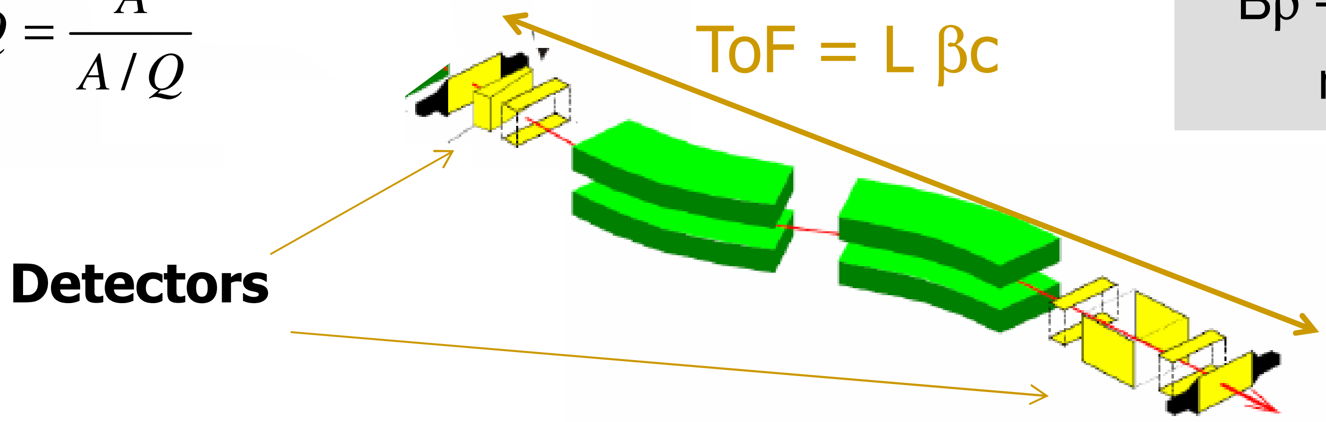

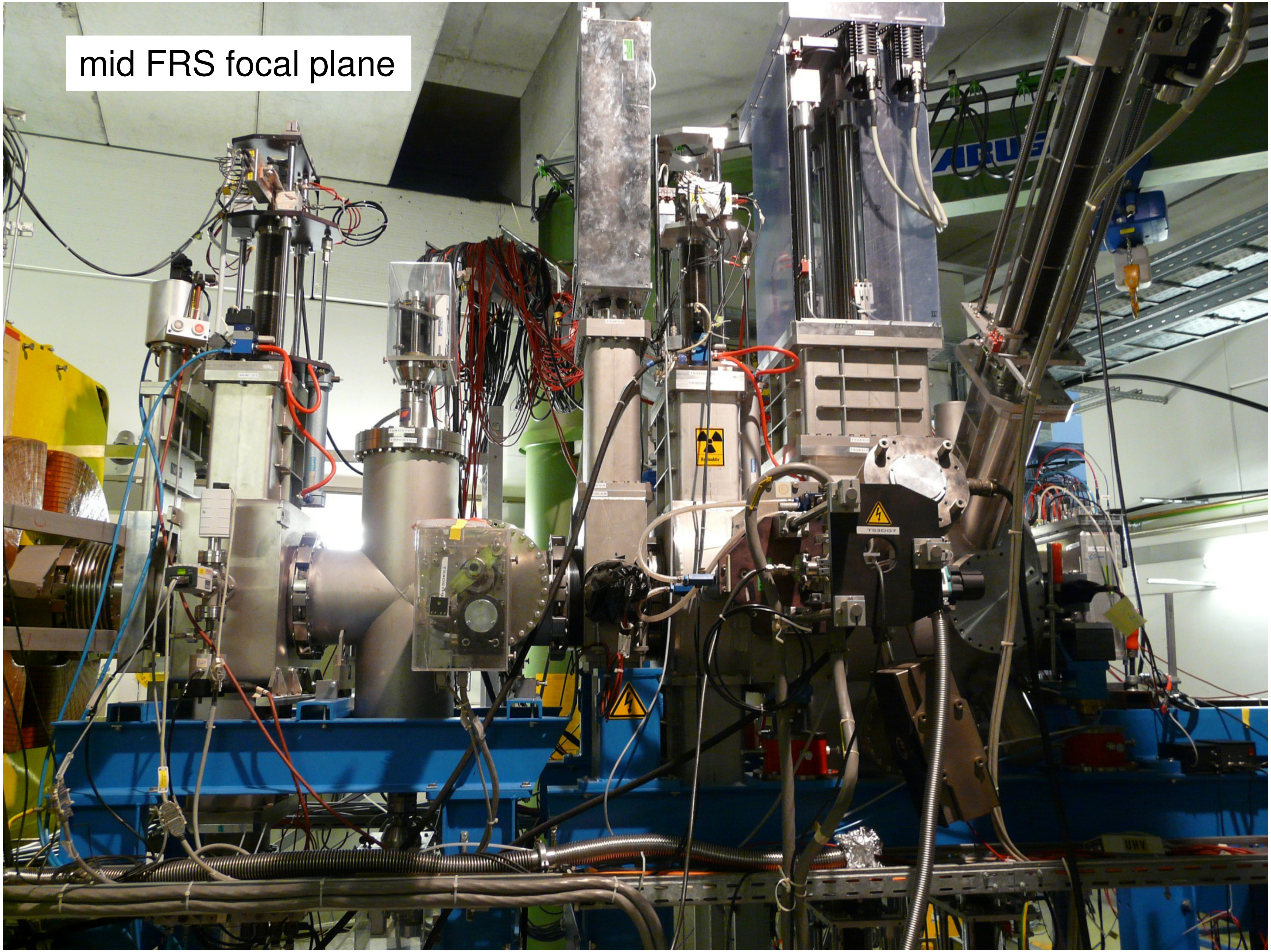
mid FRS focal plane

Discovery of 60 new isotopes

Contents lists available at SciVerse ScienceDirect

Physics Letters B

www.elsevier.com/locate/physletb

Discovery and cross-section measurement of neutron-rich isotopes in the element range from neodymium to platinum with the FRS

J. Kurcewicz[a,*], F. Farinon[a,b,1], H. Geissel[a,b], S. Pietri[a], C. Nociforo[a], A. Prochazka[a,b], H. Weick[a], J.S. Winfield[a], A. Estradé[a,c], P.R.P. Allegro[d], A. Bail[e], G. Bélier[e], J. Benlliure[f], G. Benzoni[g], M. Bunce[h], M. Bowry[h], R. Caballero-Folch[i], I. Dillmann[a,b], A. Evdokimov[a,b], J. Gerl[a], A. Gottardo[j], E. Gregor[a], R. Janik[k], A. Kelić-Heil[a], R. Knöbel[a], T. Kubo[l], Yu.A. Litvinov[a,m], E. Merchan[a,n], I. Mukha[a], F. Naqvi[a,o], M. Pfützner[a,p], M. Pomorski[p], Zs. Podolyák[h], P.H. Regan[h], B. Riese[a,b], M.V. Ricciardi[a], C. Scheidenberger[a,b], B. Sitar[k], P. Spiller[a], J. Stadlmann[a], P. Strmen[k], B. Sun[b,q], I. Szarka[k], J. Taïeb[e], S. Terashima[a,l], J.J. Valiente-Dobón[j], M. Winkler[a], Ph. Woods[r]

- $T_{1/2}$ long enough to survive for 300 ns ToF
- measured production cross sections down up to 1 pb

4 FRS settings superimposed !

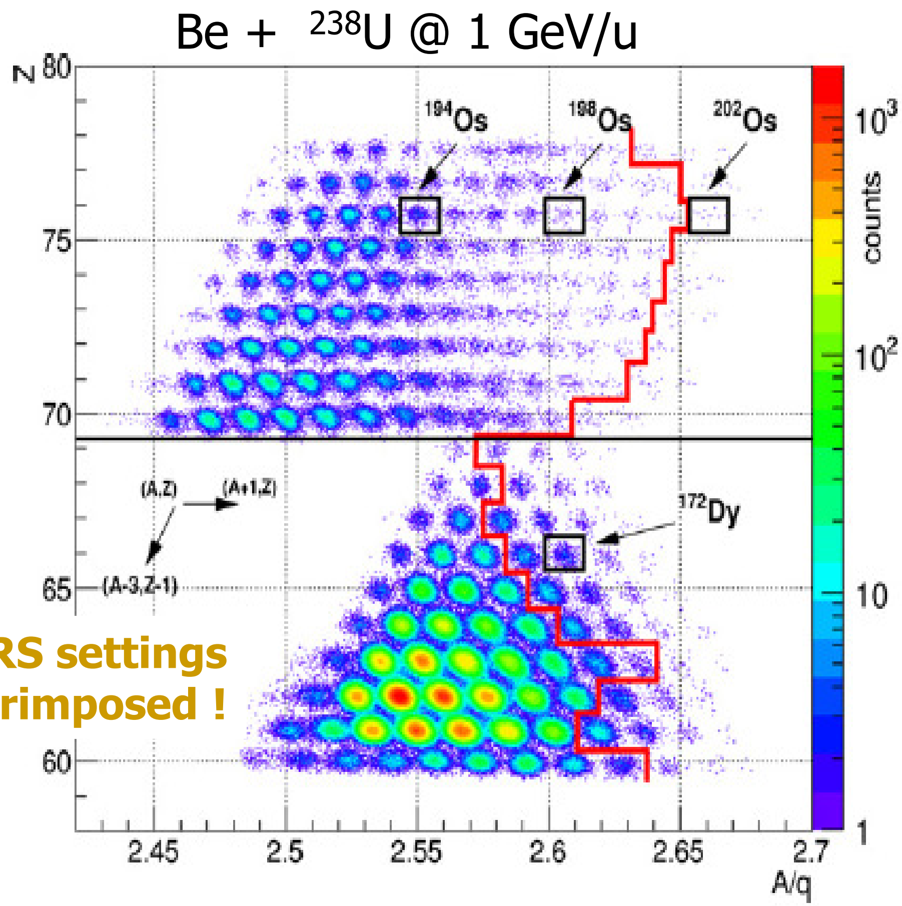

J. Kurcewicz et al., *PLB* 717 (2012) 371

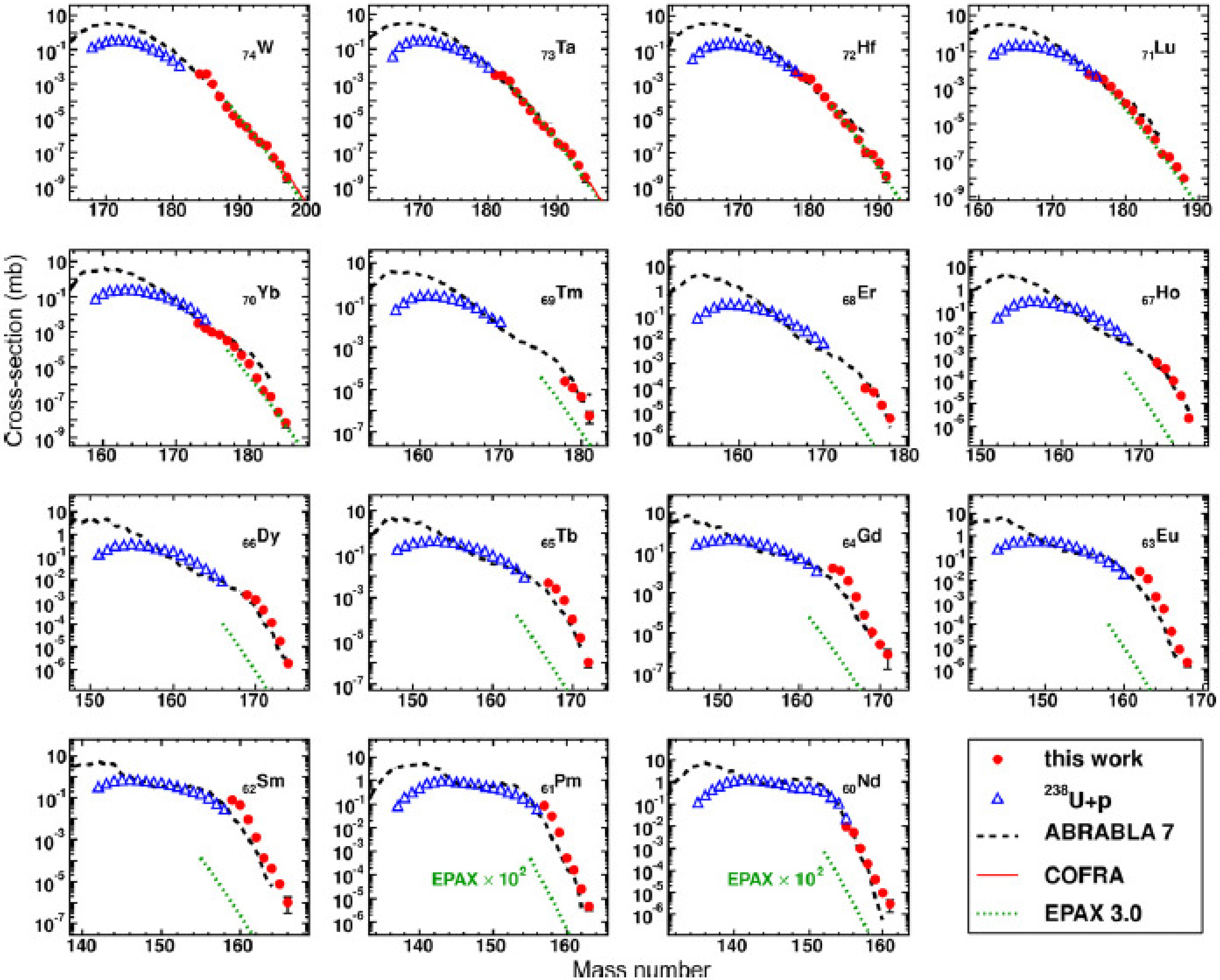

J. Kurcewicz et al., *PLB* 717 (2012) 371

^{100}Sn study

ARTICLE C.B. Hinke et al., *Nature* 486 (2012) 341

doi:10.1038/nature11116

Superallowed Gamow–Teller decay of the doubly magic nucleus ^{100}Sn

C. B. Hinke[1], M. Böhmer[1], P. Boutachkov[2], T. Faestermann[1], H. Geissel[2], J. Gerl[2], R. Gernhäuser[1], M. Górska[2], A. Gottardo[3], H. Grawe[2], J. L. Grębosz[4], R. Krücken[1,5], N. Kurz[2], Z. Liu[6], L. Maier[1], F. Nowacki[7], S. Pietri[2], Zs. Podolyák[8], K. Sieja[7], K. Steiger[1], K. Straub[1], H. Weick[2], H.-J. Wollersheim[2], P. J. Woods[6], N. Al-Dahan[8], N. Alkhomashi[8], A. Ataç[9], A. Blazhev[10], N. F. Braun[10], I. T. Čeliković[11], T. Davinson[6], I. Dillmann[2], C. Domingo-Pardo[12], P. C. Doornenbal[13], G. de France[14], G. F. Farrelly[8], F. Farinon[2], N. Goel[2], T. C. Habermann[2], R. Hoischen[2], R. Janik[15], M. Karny[16], A. Kaşkaş[9], I. M. Kojouharov[2], Th. Kröll[17], Y. Litvinov[2], S. Myalski[4], F. Nebel[1], S. Nishimura[13], C. Nociforo[2], J. Nyberg[18], A. R. Parikh[19], A. Procházka[2], P. H. Regan[8], C. Rigollet[20], H. Schaffner[2], C. Scheidenberger[2], S. Schwertel[1], P.-A. Söderström[13], S. J. Steer[8], A. Stolz[21] & P. Strmeň[15]

Be + ^{124}Xe @ 1 GeV/u

≤ 1 ^{100}Sn/hour !

- measured $T_{1/2}$, β-decay end-point energy, GT strength, the largest so far measured in allowed nuclear β-decay, establishing the 'superallowed' nature of this pure spin-flip ^{100}Sn $(0^+) \rightarrow$ ^{100}In $(1^+ (\pi g_{9/2}^{-1}, \nu g_{7/2}))$ transition

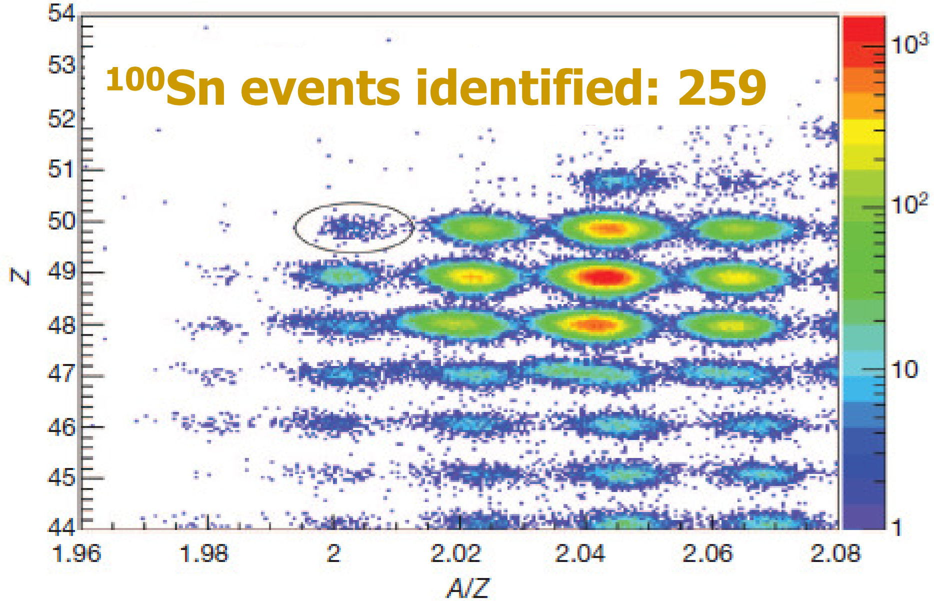

Access to r-process nuclei
N=82 and N=126

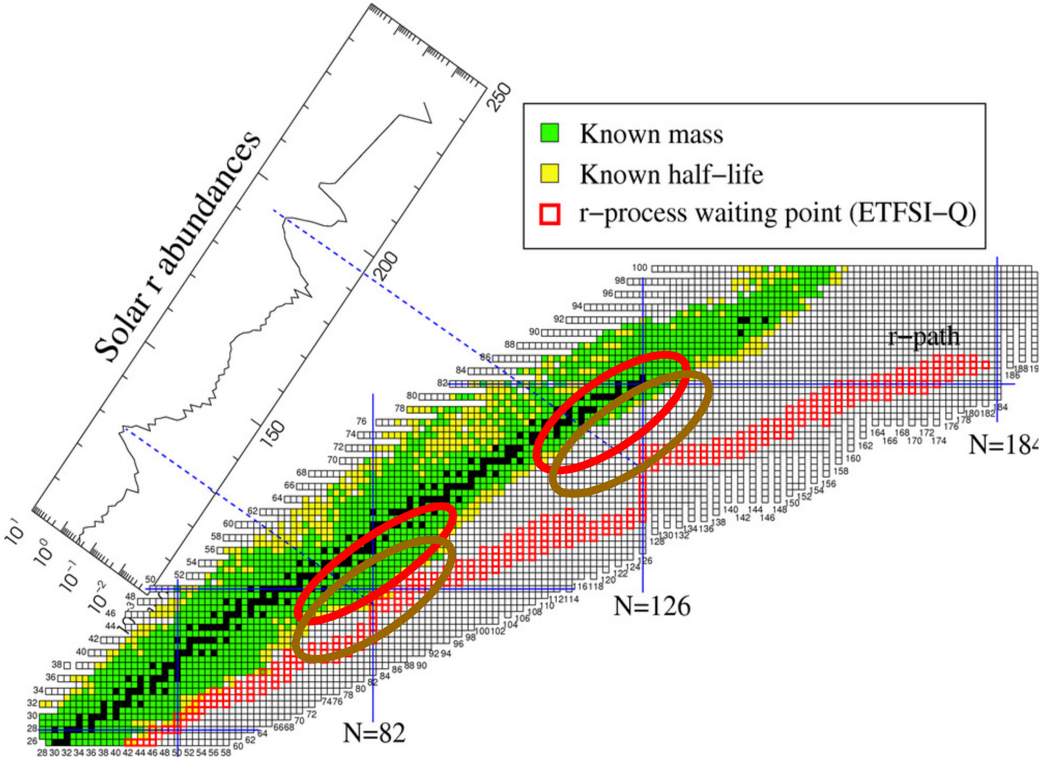

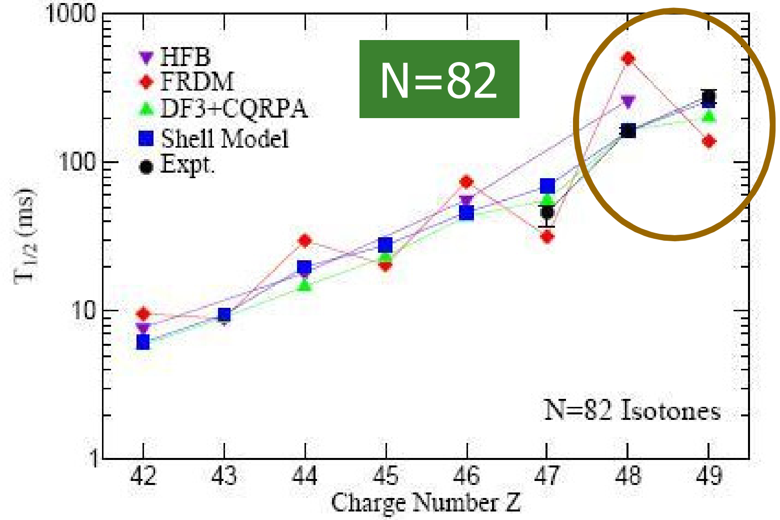

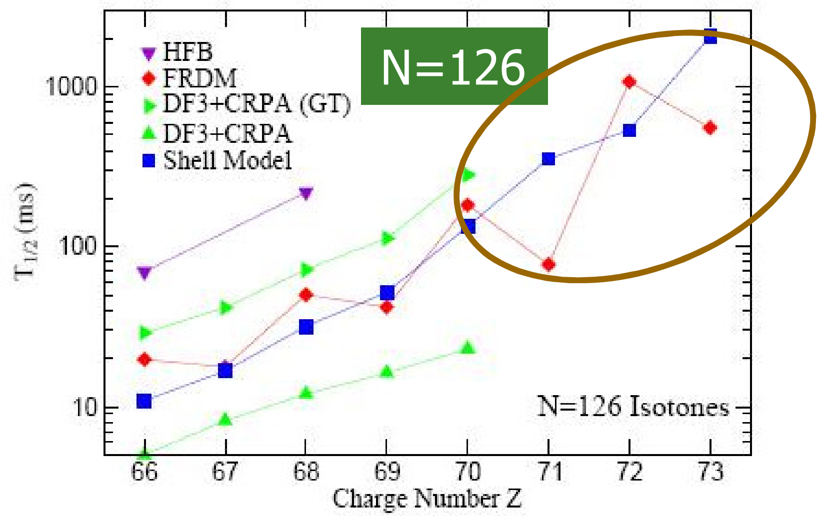

Masses (MATS)
Lifetimes (DESPEC)

H. Grawe, K. Langanke and G. Martínez-Pinedo
Rep. Prog. Phys. 70 No 9 (September 2007) 1525

FAIR: Facility for Antiproton and Ion Research

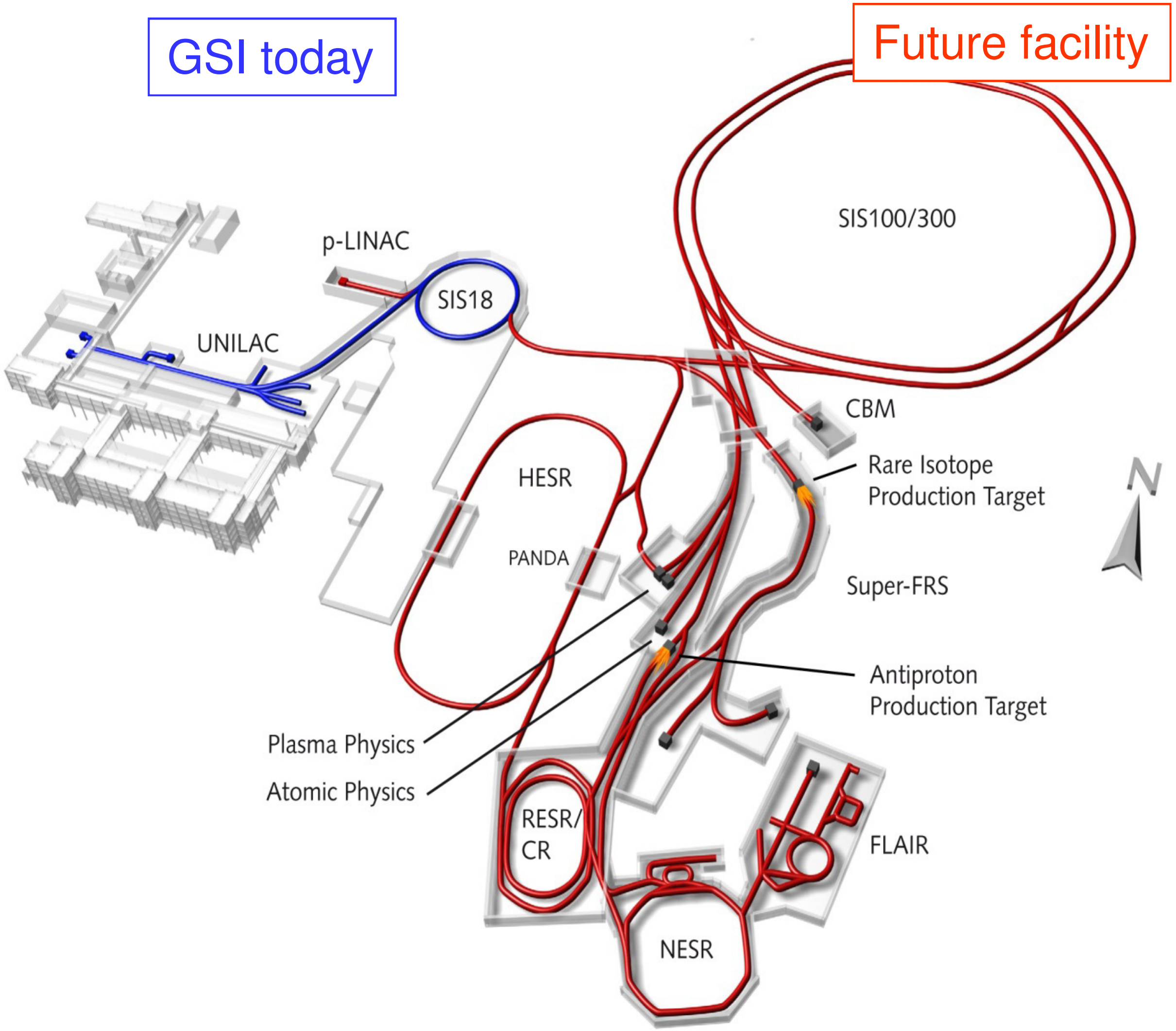

$B\rho$ = 100 Tm :
29 GeV protons
for pbar production;
2.716 GeV/u $^{238}U^{28+}$

$B\rho$ = 300 Tm :
34 GeV/u $^{238}U^{92+}$ for
heavy ion collisions

Time structure:
pulsed (50-90ns)
quasi DC (SIS-300)

NUSTAR facility at FAIR

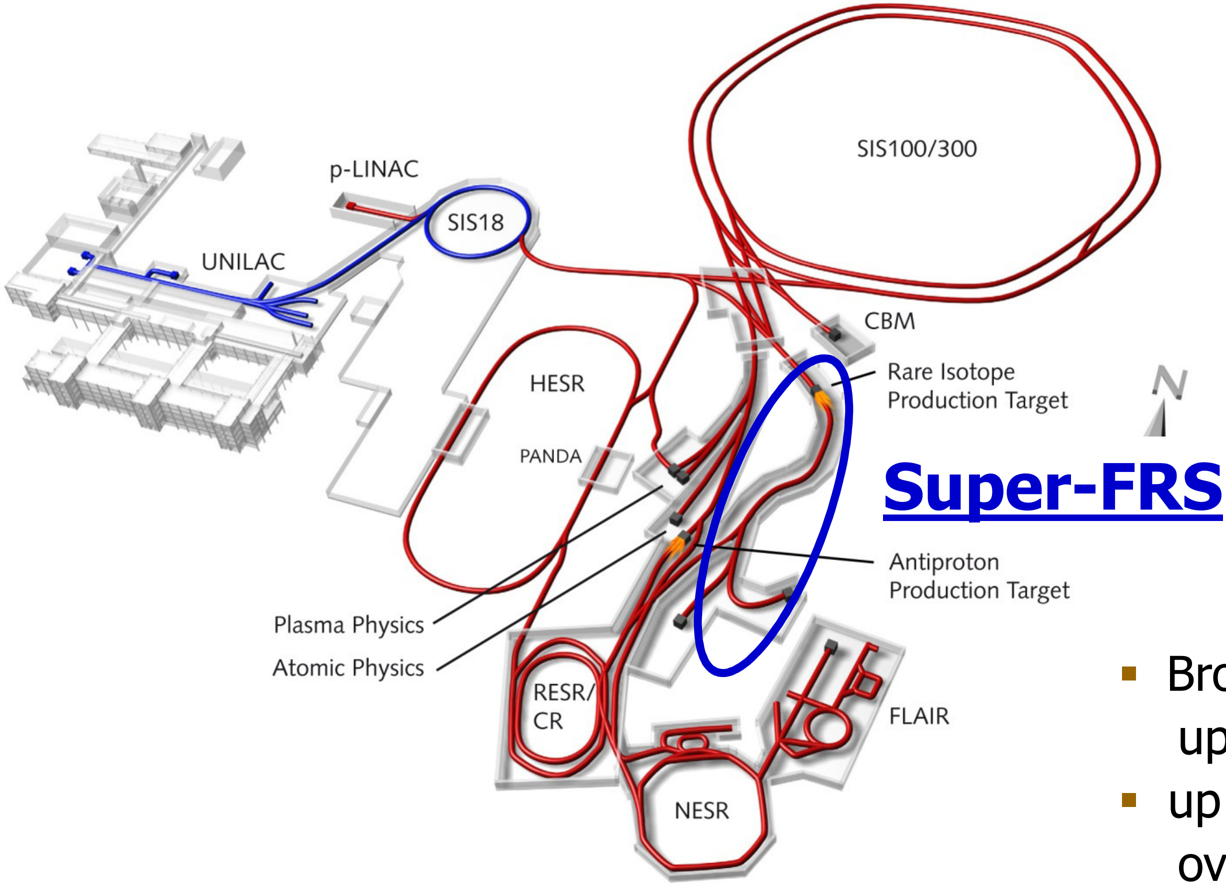

Primary Beams

- **$5 \cdot 10^{11}$ $^{238}U^{28+}$/s @1.5-2 GeV/u**
- factor **100-1000** in intensity over present

Secondary Beams

- Broad range of radioactive beams up to **1.5 - 2 GeV/u**
- up to factor **10 000** in intensity over present

Available intensities determine the type/detail of studies that can be performed

Layout and design parameter of the Super-FRS

Projectile:
- Elements p - U
- Energy up to 1.5 GeV/u
- Intensity up to 10^{12} /s (depending on element)
- DC or pulsed operation

Design Parameters:

$\varepsilon_x = \varepsilon_y =$ 40 π mm mrad

$\Phi_x = \pm 40$ mrad

$\Phi_y = \pm 20$ mrad

$\Delta P/P = \pm 2.5$ %

$B\rho$ = 2 - 20 Tm

R_{ion} = 750 / 1500 (first / second stage)

Spot size on target

σ_x = 1.0 mm

σ_y = 2.0 mm

Secondary beams:

RIB up to 1.5 GeV/u

up to factor 10000 in intensity

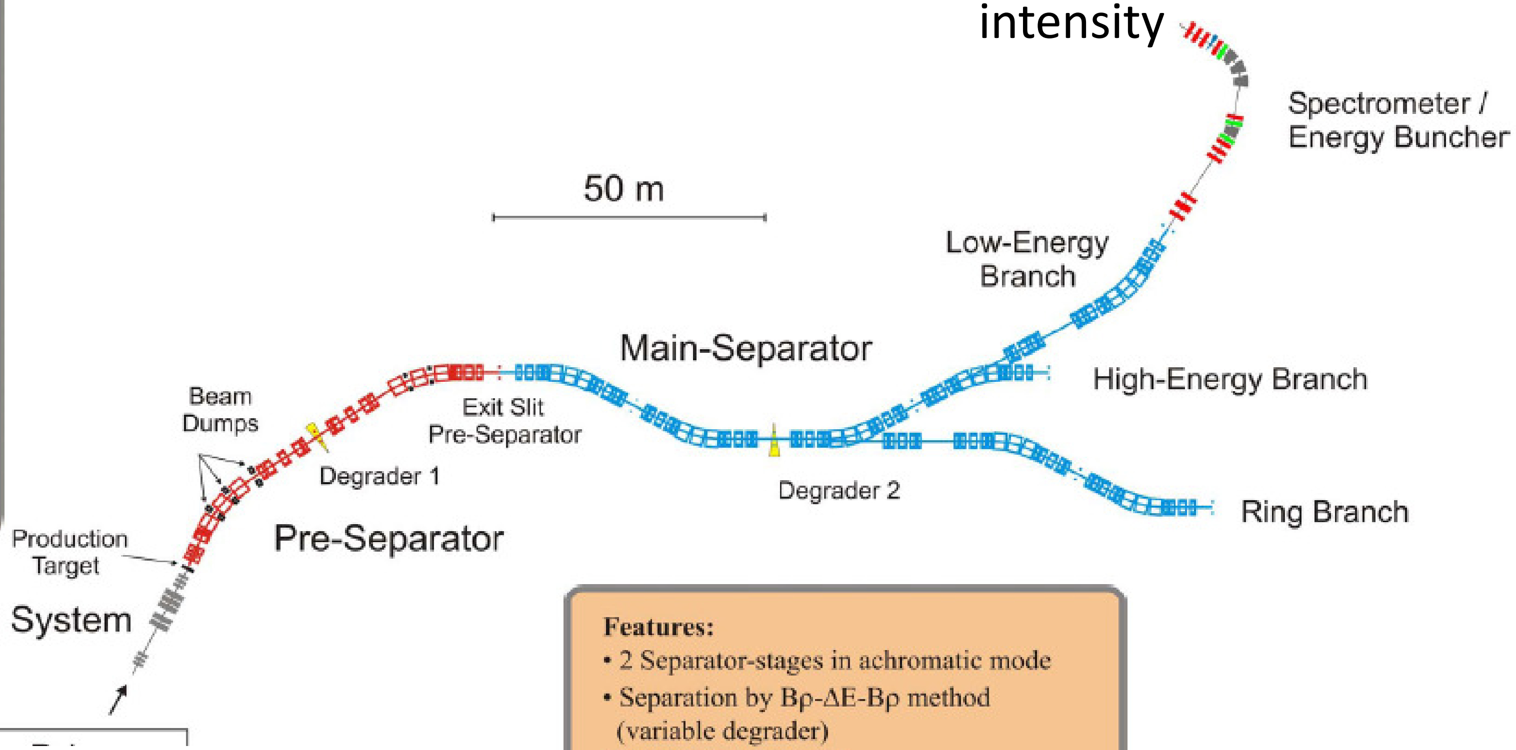

Features:
- 2 Separator-stages in achromatic mode
- Separation by $B\rho$-ΔE-$B\rho$ method (variable degrader)
- Multi-branch system
- Large acceptance utilizing sc magnets
- Handling concept for high- radiation area

Primary beams:

$3.5 \cdot 10^{11}$ ^{238}U/s up to 1.5 GeV/u

factor 100-1000 in intensity

Martin Winkler, Annual NuSTAR Meeting, GSI, March.3–5, 2010

Parameters of the Super-FRS

Comparison FRS - Super-FRS

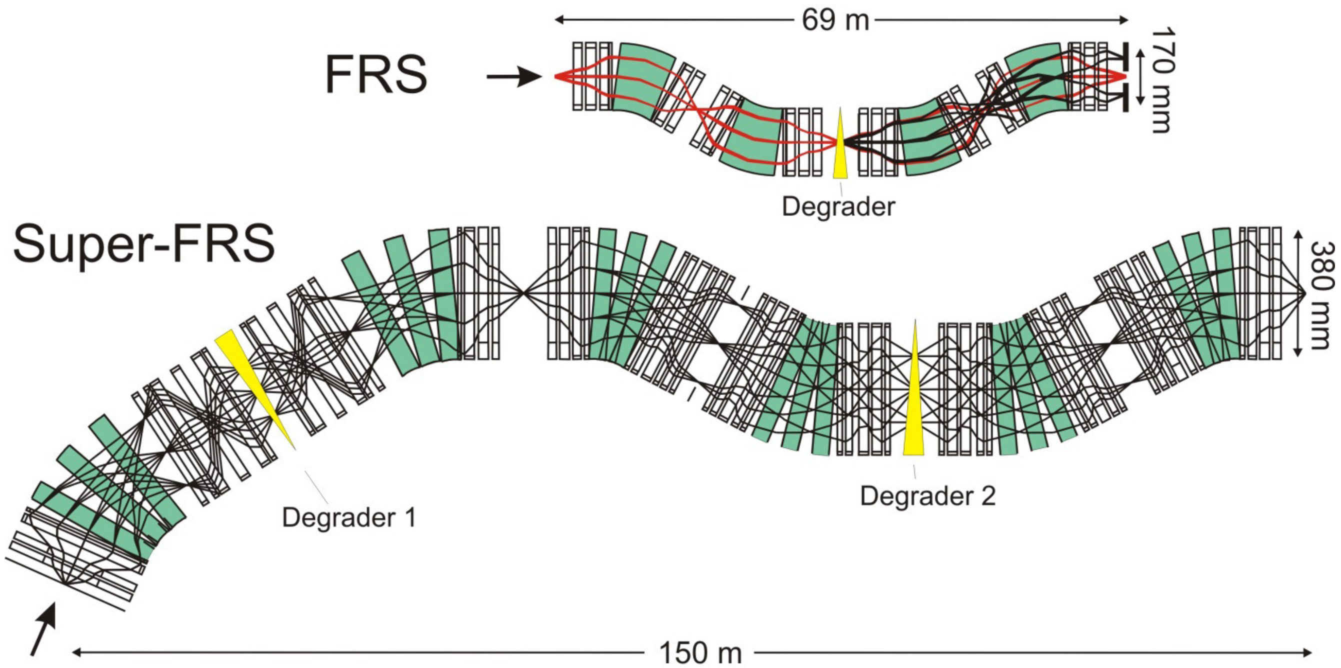

	$B\rho_{max}$	$\Delta p/p$	$\Delta\theta/\theta$, $\Delta\phi/\phi$	Resolving Power
Super-FRS	20 Tm	±2.5 %	±40, ±20 mr	1500 (40πmm mr)
FRS	18 Tm	±1%	±7.5, ±7.5 mr	1500 (20πmm mr)

Comparison FRS – Super-FRS

Transmission gain

- Fragmentation

$^{124}Xe + C \rightarrow {}^{100}Sn$

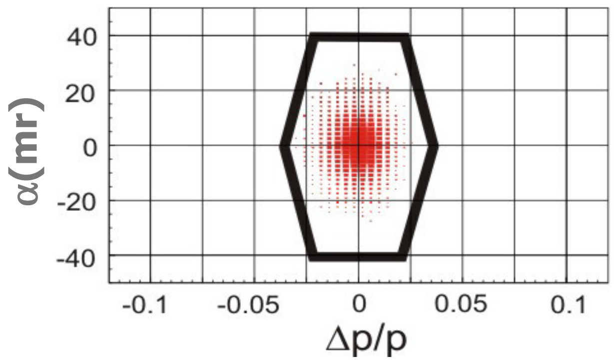

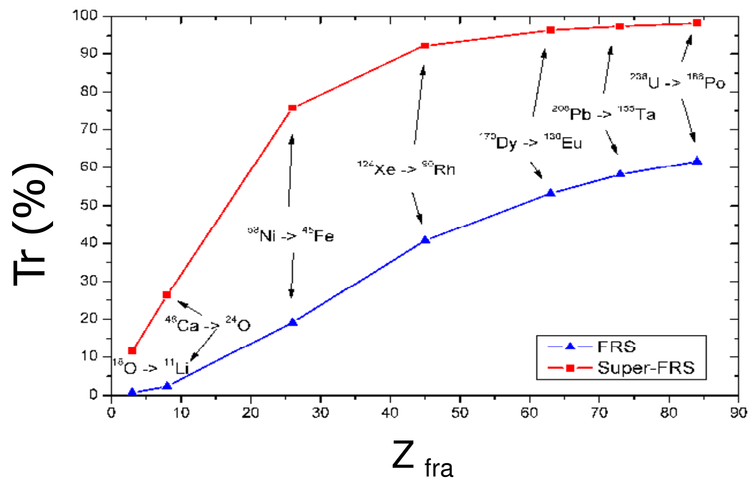

- Fission

$^{238}U + C \rightarrow {}^{78}Ni$

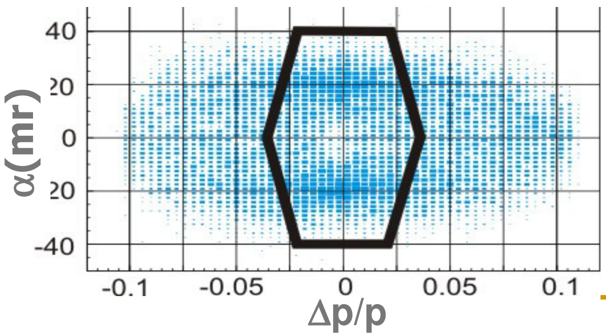

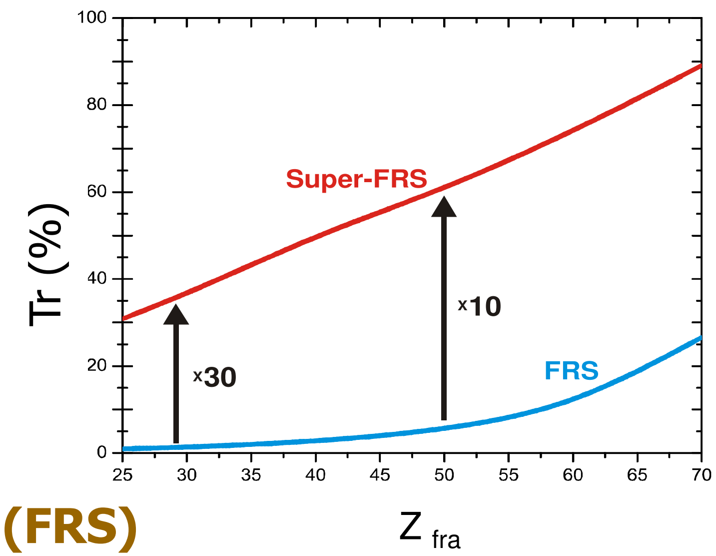

Apertures (Super-FRS) ≈ 2 x Apertures (FRS)

2-stage separation
e.g. ^{100}Sn

1-stage separator 2-stage separator

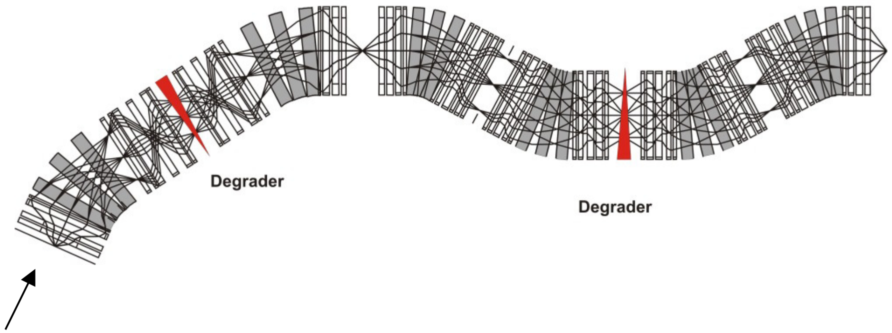

Fragmentation of ^{124}Xe @ 1 GeV/u

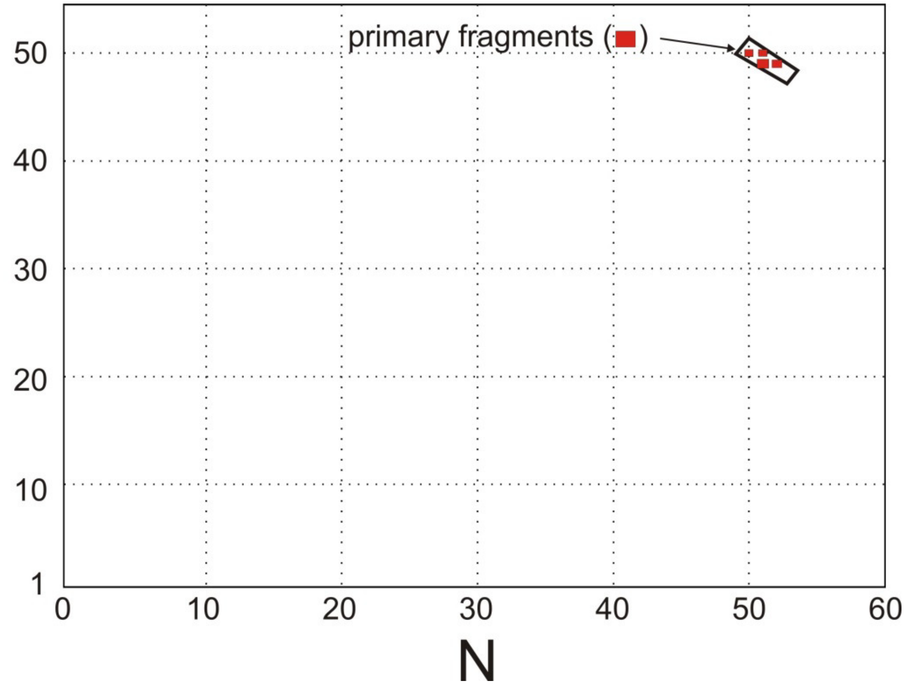

- Strong reduction of contaminants
- Optimization of fragment rate
- Main separator used for secondary reaction studies

Advantages of high-energy RIBs

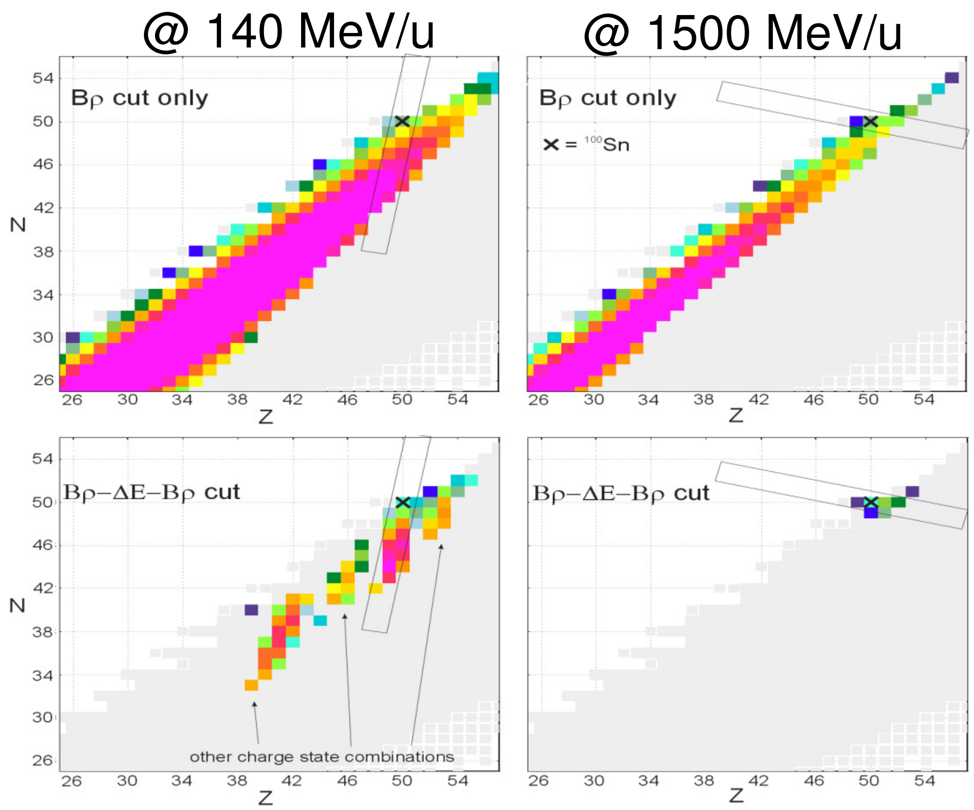

- Thick production target – very exotic RIBs
- Pure incoming RIBs incident on secondary target
- Fully stripped reaction products after secondary target
- Strong kinematical forward focusing of reaction products
- High luminosity – thick reaction target

Future requirements

- Increasing intensity of radioactive beams

  requires new developments in detecting system & electronics

- Clean full isotope identification on event-by-event basis (PID)

  → momentum tagging $\Delta x \sim 1mm$

  → ToF measurements $\Delta ToF \sim 100ps$ (FWHM) **A > 150**

Isotope identification

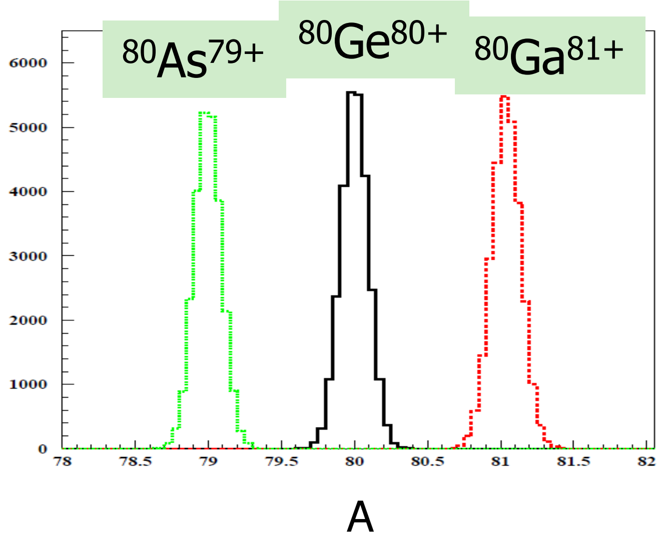

fragmentation $^{86}Kr + C \rightarrow$ ^{80}Ge

Monte Carlo simulations

Yields not scaled

σ_t= 30ps, σ_x= 0.5mm

MOCADI code

(http://web-docs.gsi.de/~weick/mocadi/)

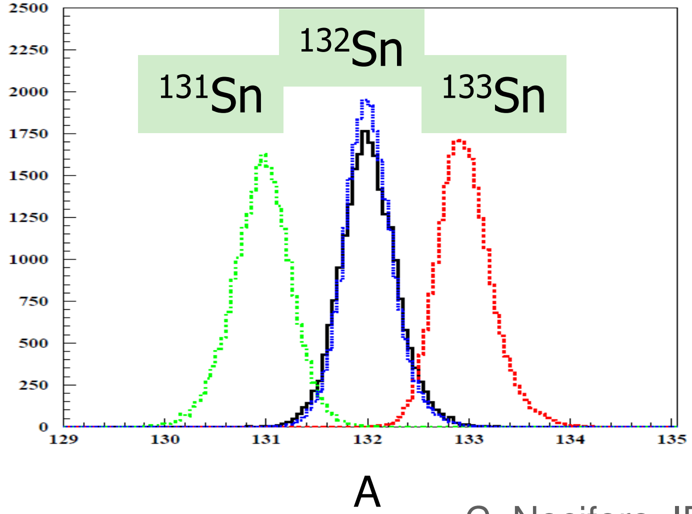

fission $^{238}U + C \rightarrow$ ^{132}Sn

Resolution

MOCADI simulations

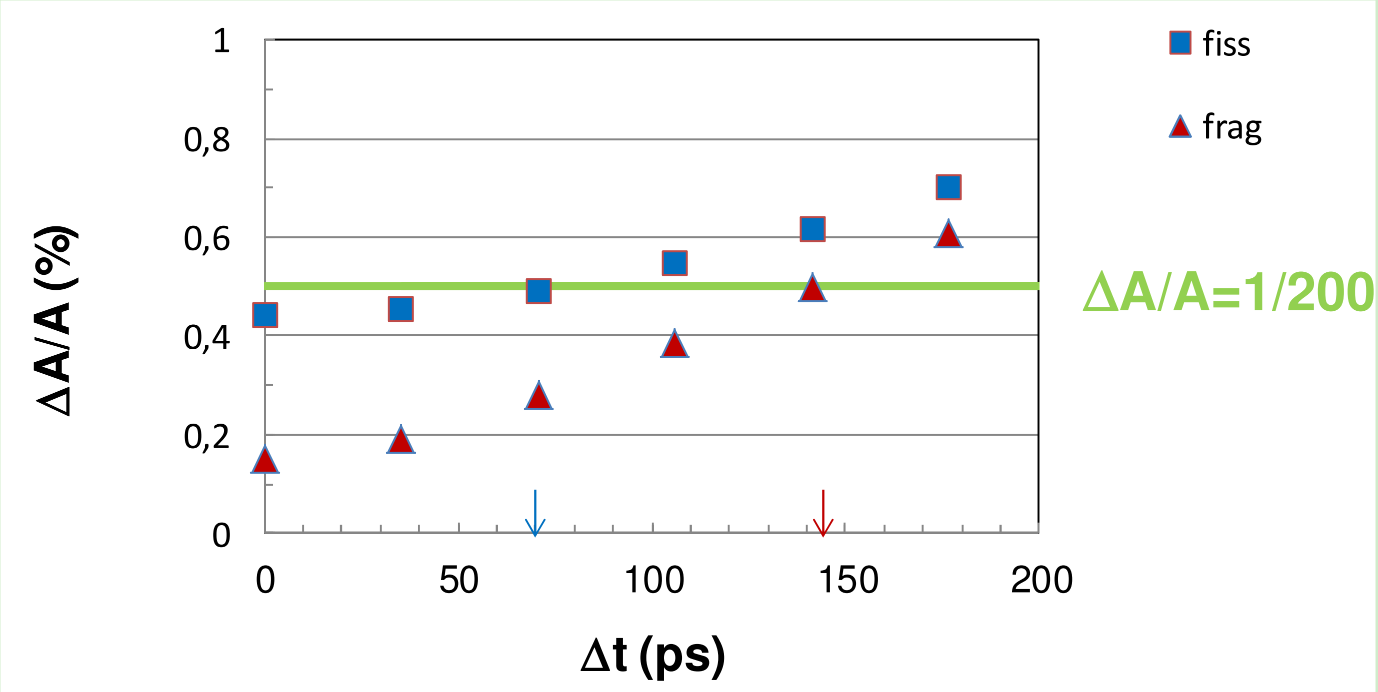

Ion optics (no target, no degraders)

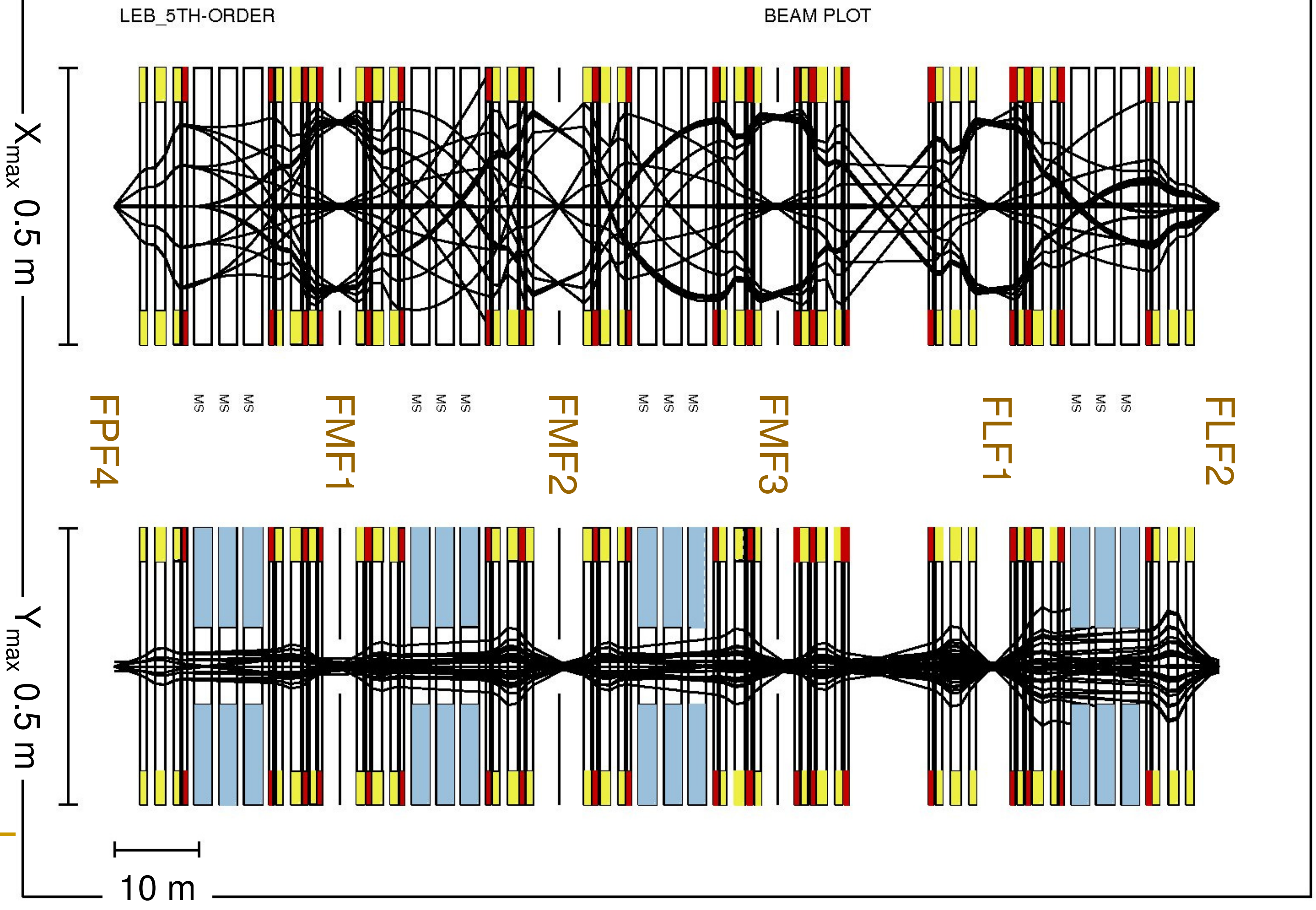

Detector sizes at focal planes

Dipole gaps: 170 mm

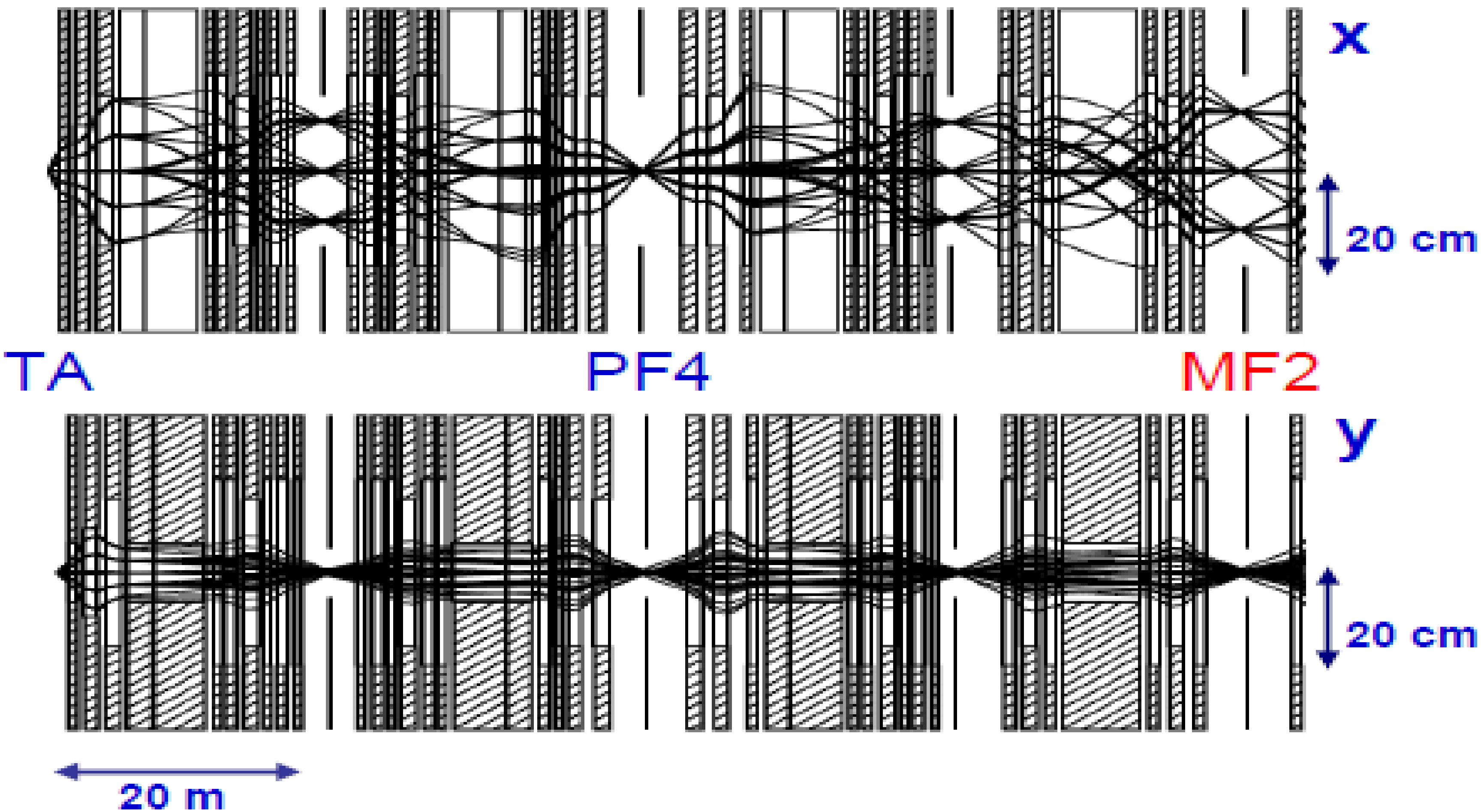

Particle interaction with matter

The energy loss for a charged (*z*) particle crossing a medium (Z, A) *dx* is:

$$-\frac{dE}{dx} = K z^2 \frac{Z}{A}\frac{1}{\beta^2} L(\beta) \qquad (*)$$

where $K/A = 4\pi N_A r_e^2 m_e c^2 = 0.307075\ MeV\,g^{-1}cm^2,$

with m_e and r_e the electron mass and classical radius,
N_A is the Avogadro´s number.

The parameter $L(\beta) = L_0(\beta) + \cancel{\sum_i \Delta L_i}$

where $$L_0(\beta) = ln\left(\frac{2m_e c^2\beta^2\gamma^2 T_{max}}{I^2}\right) - \beta^2 - \frac{\delta(\beta\gamma)}{2}$$

$$with\ \ \gamma = \frac{E_{kin} + m_0c^2}{m_0c^2}\quad and\ \ \beta = \sqrt{1 - 1/\gamma^2}$$

with T_{max} the maximum kinetic energy transferred to a free electron in a single collision, I the mean excitation energy and δ the density correction.

Neglecting $\sum_i \Delta L_i$ (*) is the Bethe-Bloch equation.

Particle interaction with matter (II)

At non-relativistic energies the ionization energy loss has 1/β^2 energy dependence, whereas at relativistic energies the energy loss is slightly growing.
It has a minimum at a certain energy; a particle with this energy is called a ´minimum ionizing particle´ (MIP). The Bethe-Bloch formula describes quite precisely the energy losses of projectile z=1, however it fails applied to heavy ions at both low and high energies. Therefore, further corrections $\sum_i \Delta L_i$ must be applied.

Lindhard-Sørensen (LS) correction takes into account a finite nuclear size.

At E_{kin} > 500 MeV/u the expression derived for point-like ions is valid:

$$\Delta L_{LS} = \sum_{k=1}^{\infty}\left[\frac{k}{\eta^2}\frac{k-1}{2k-1}sin^2(\delta_k - \delta_{k-1}) + \frac{k}{\eta^2}\frac{k+1}{2k+1}sin^2(\delta_{-k} - \delta{-k}-1) + \frac{k}{4k^2-1}\frac{1}{\gamma^2k^2+\eta^2} - \frac{1}{k}\right] + \frac{\beta^2}{2}$$

where $\eta = \alpha z/\beta$, with α the fine structure constant, δ_k the relativistic Coulomb phase shift and k a parameter used in the summation over the partial waves.

Stopping power in Al degrader

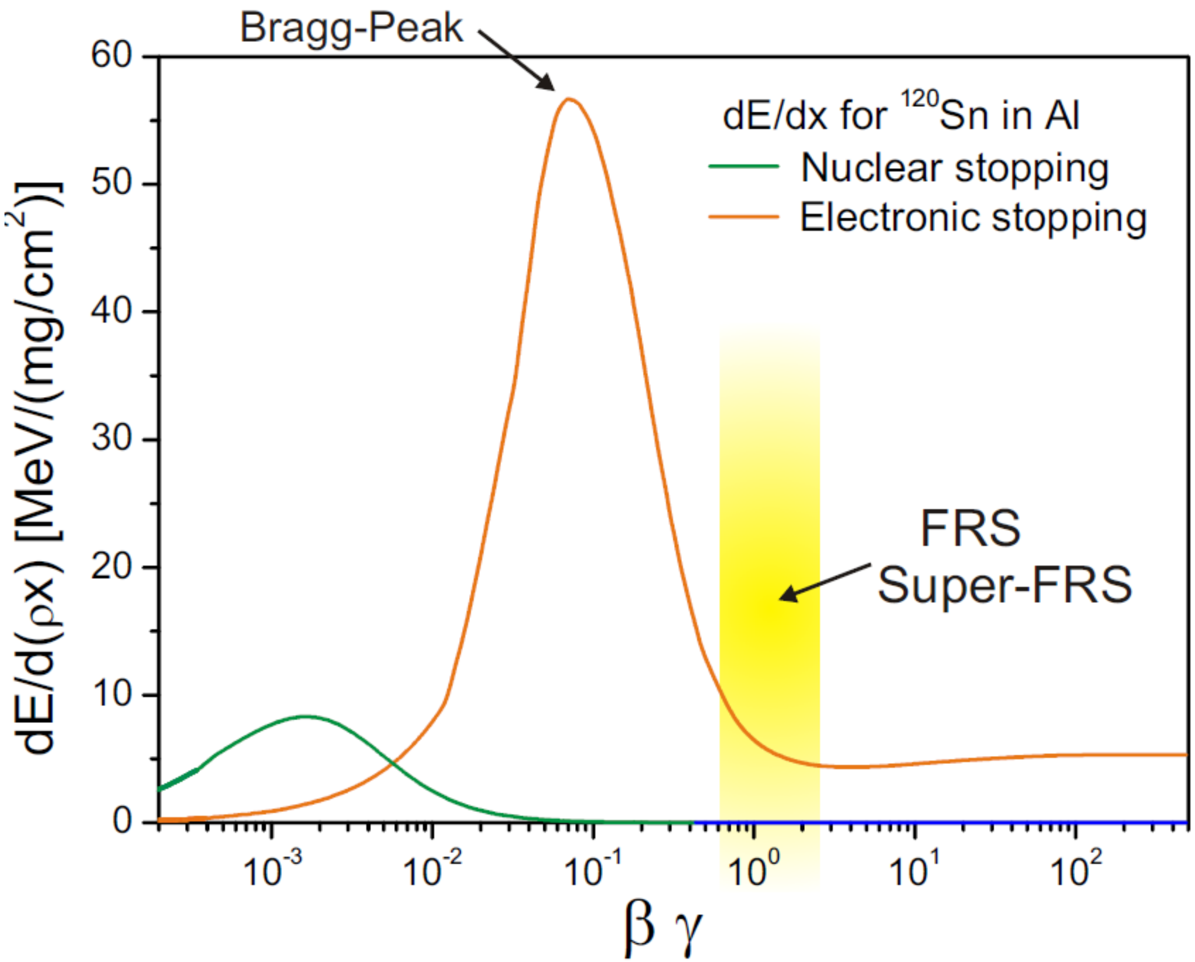

Particle interaction with matter

The LS correction gives perfect agreement with the experimental data for bare projectiles. At lower energies the heavy ions are no longer completely stripped. Therefore, *z* is replaced by the effective charge

$$q_{eff} = z\left[1 - exp\left(\frac{-0.95v}{z^{\frac{2}{3}}v_0}\right)\right]$$

where v_0 is the Bohr velocity.